New Limits on Coupling of Fundamental Constants to Gravity Using ^{87}Sr Optical Lattice Clocks

S. Blatt,* A. D. Ludlow, G. K. Campbell, J. W. Thomsen,† T. Zelevinsky,‡ M. M. Boyd, and J. Ye
JILA, National Institute of Standards and Technology and University of Colorado, Department of Physics, University of Colorado, Boulder, CO, 80309-0440, USA

X. Baillard, M. Fouché,§ R. Le Targat, A. Brusch,¶ and P. Lemonde
LNE-SYRTE, Observatoire de Paris, 61, avenue de l'Observatoire, 75014, Paris, France

M. Takamoto, F.-L. Hong,** and H. Katori
Department of Applied Physics, Graduate School of Engineering, The University of Tokyo, Bunkyo-ku, 113-8656 Tokyo, Japan

V. V. Flambaum
School of Physics, The University of New South Wales, Sydney NSW 2052, Australia
(Dated: April 29, 2008)

The $^1S_0$-$^3P_0$ clock transition frequency $\nu_{\rm Sr}$ in neutral ^{87}Sr has been measured relative to the Cs standard by three independent laboratories in Boulder, Paris, and Tokyo over the last three years. The agreement on the 1×10^{-15} level makes $\nu_{\rm Sr}$ the best agreed-upon optical atomic frequency. We combine periodic variations in the ^{87}Sr clock frequency with ^{199}Hg$^+$ and H-maser data to test Local Position Invariance by obtaining the strongest limits to date on gravitational-coupling coefficients for the fine-structure constant α, electron-proton mass ratio μ and light quark mass. Furthermore, after ^{199}Hg$^+$, ^{171}Yb$^+$ and H, we add ^{87}Sr as the fourth optical atomic clock species to enhance constraints on yearly drifts of α and μ.

PACS numbers: 42.62.Eh, 06.20.Jr, 32.30.Jc, 06.30.Ft

Frequency is the physical quantity that has been measured with the highest accuracy. While the second is still defined in terms of the radio-frequency hyperfine transition of ^{133}Cs, the higher precision and lower systematic uncertainty achieved in recent years with optical frequency standards promises tests of fundamental physics concepts with increased resolution. For example, some cosmological models imply that fundamental constants and thus atomic frequencies had different values in the early universe, suggesting that they might still be changing. Records of atomic clock frequencies measured against the Cs standard can be analyzed [1, 2] to obtain upper limits on present-day variations of fundamental constants such as the fine-structure constant $\alpha = e^2/(4\pi\epsilon_0\hbar c)$ or the electron-proton mass ratio $\mu = m_e/m_p$ [3, 4, 5, 6, 7]. Some unification theories imply violation of Local Position Invariance by predicting coupling of these constants to the ambient gravitational field. Such a dependence could be tested with a deep-space clock mission [8], but would also be observable in the frequency record of earth-bound clocks as Earth's elliptic orbit takes the clock through a varying solar gravitational potential [9]. Annual changes in clock frequencies can thus constrain gravitational coupling of fundamental constants [7, 10, 11]. Good constraints obtained from such analyses require high confidence in the data and a fast sampling rate. However, a full evaluation of an atomic clock system takes several days so that high-accuracy frequency data is naturally sparse.

Three laboratories have measured the doubly forbidden ^{87}Sr $^1S_0$-$^3P_0$ intercombination line at $\nu_{\rm Sr}$ = 429 228 004 229 874 Hz with high accuracy over the last three years. These independent laboratories in Boulder (USA), Paris (France), and Tokyo (Japan) agree at the level of 1.7 Hz [12, 13, 14, 15]. The agreement between Boulder and Paris is 1×10^{-15} [12, 13, 14], approaching the Cs limit, which speaks for the Sr lattice clock system as a candidate for future redefinition of the SI second and makes $\nu_{\rm Sr}$ the best agreed-upon optical clock frequency. In this paper, we analyze the international Sr frequency record for long-term variations and combine our results with data from other atomic clock species to obtain the strongest limits to date on coupling of fundamental constants to gravity. In addition, our data contributes a high-accuracy measurement of an optical atomic clock species, which itself has low sensitivity to variation in fundamental constants, to the search for drifts of fundamental constants, improving confidence in the null result at the current level of accuracy.

In a strontium lattice clock, neutral fermionic ^{87}Sr atoms are trapped at the anti-nodes of a vertical one-dimensional optical lattice at the Stark-cancellation wavelength, creating an ensemble of nearly identical quantum absorbers at μK temperatures. The $^1S_0$-$^3P_0$ clock transition [16] is interrogated with a highly frequency-stabilized 698 nm spectroscopy laser in the re-

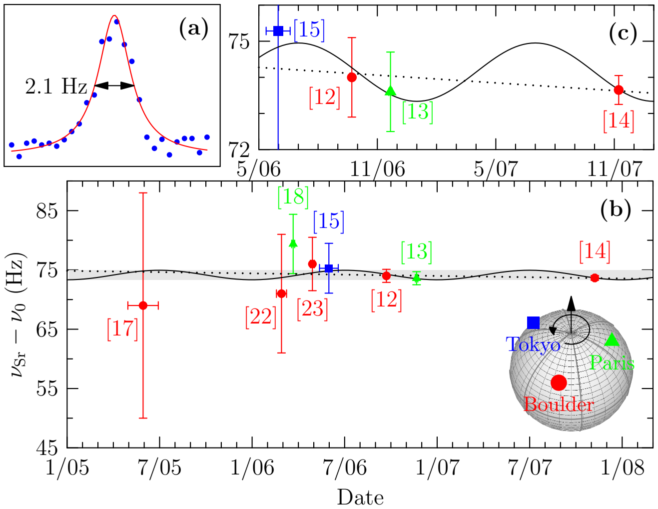

FIG. 1: (color online). (a) Spectrum of the ^{87}Sr ^{1}S$_0$-^{3}P$_0$ clock transition with quality factor 2×10^{14}. (b) Measurements of clock transition from JILA (red circle), SYRTE (green triangle), and U. Tokyo (blue square) over the last 3 years. Frequency data is shown relative to $\nu_0 = 429\,228\,004\,229\,800$ Hz. Weighted linear (dotted line) and sinusoidal (solid line) fits determine a yearly drift rate and an amplitude of annual variation. (c) Zoom into the four most recent measurements, showing agreement within 1.7 Hz and giving the dominant contribution to both drift and annual variation.

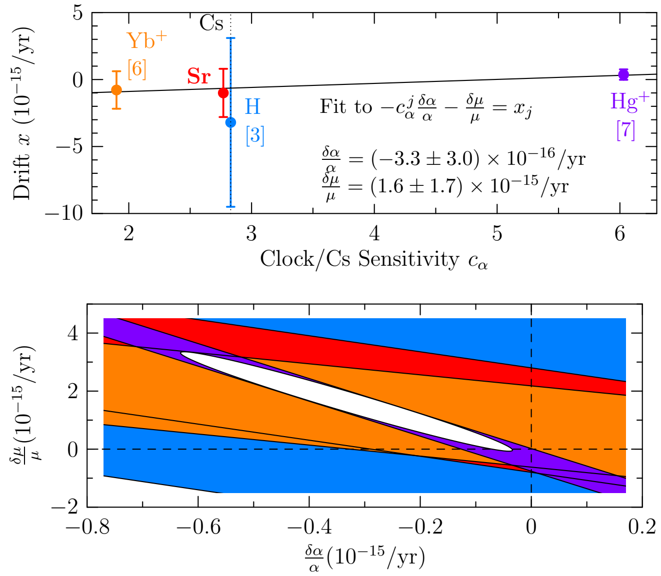

FIG. 2: (color online). The upper panel shows fractional frequency drifts for ^{171}Yb$^+$ (orange), ^{87}Sr (red), H 1S-2S (blue) and ^{199}Hg$^+$ (purple) versus their sensitivity to α-variation relative to Cs. Sensitivity due to Cs is indicated as a dotted vertical line. A linear fit (solid line) determines yearly drift rates $\delta\alpha/\alpha$ and $\delta\mu/\mu$. The drift rate constraints from each species are shown in the lower panel as respectively colored bars. The fit determines a confidence ellipse (white) [3, 6, 7] with projections equal to the parameters' 1-σ uncertainties.

solved sideband limit and the Lamb-Dicke regime [12, 13, 14, 15, 17, 18]. Using individual magnetic sublevels, spectra with quality factors of $> 2 \times 10^{14}$ have been recovered [19] as shown in Fig. 1(a). This high-resolution spectroscopy afforded by the optical lattice allows measurement of the clock frequency with high accuracy and evaluation of systematic uncertainties at one part in 10^{16}, limited by blackbody and residual density effects [20]. Spectroscopic information from the atomic sample is used to steer the laser to match the clock transition frequency, which is then measured relative to the Cs standard using an octave-spanning optical frequency comb [21].

In combination with data from other optical atomic clock species, variations in the measured Sr clock frequency can constrain variation of fundamental constants. It is necessary to analyze a diverse selection of atomic species to rule out species-dependent systematic effects and test the broad predictions of the underlying relativistic theory. We will introduce the formalism required to constrain the coupling to gravity by first analyzing the global frequency record for linear drifts in α and μ.

Figure 1(b) displays Sr clock frequency measurements since 2005. The frequency uncertainties are based on values from references [12, 13, 14, 15, 17, 18, 22, 23]. The date error bar indicates the time interval over which each measurement took place. A weighted linear fit (dotted line) results in a frequency drift of $(-1.0 \pm 1.8) \times 10^{-15}$/yr, mostly determined by the difference between the last three high-accuracy measurements [12, 13, 14]. This yearly drift can be related to a drift of fundamental constants via relativistic sensitivity constants $K_{\rm rel}$. Values for various clock transitions of interest have been calculated in references [24, 25] and the fractional frequency variation of an optical transition can be written as

$$\frac{\delta\nu_{\rm opt}}{\nu_{\rm opt}} = K^{\rm opt}_{\rm rel}\frac{\delta\alpha}{\alpha}. \tag{1}$$

The Cs standard operates on a hyperfine transition, which is also sensitive to variations in μ. For a hyperfine transition, the above equation is modified to

$$\frac{\delta\nu_{\rm hfs}}{\nu_{\rm hfs}} = (K^{\rm hfs}_{\rm rel} + 2)\frac{\delta\alpha}{\alpha} + \frac{\delta\mu}{\mu}. \tag{2}$$

Here, the change in μ arises from variations in the nuclear magnetic moment of the Cs atom [25]. The following drift analysis will focus on optical clocks measured against Cs, since inclusion of hyperfine clock data from Rb/Cs [5, 26] does not change the results significantly.

The overall fractional frequency variation x_j of an optical clock species j compared to Cs can be related to variation of α and μ as

$$\begin{aligned} x_j \equiv \frac{\delta(\nu_j/\nu_{\rm Cs})}{\nu_j/\nu_{\rm Cs}} &= \left(K^j_{\rm rel} - K^{\rm Cs}_{\rm rel} - 2\right)\frac{\delta\alpha}{\alpha} - \frac{\delta\mu}{\mu} \\ &\equiv -c^j_\alpha\frac{\delta\alpha}{\alpha} - \frac{\delta\mu}{\mu}. \end{aligned} \tag{3}$$

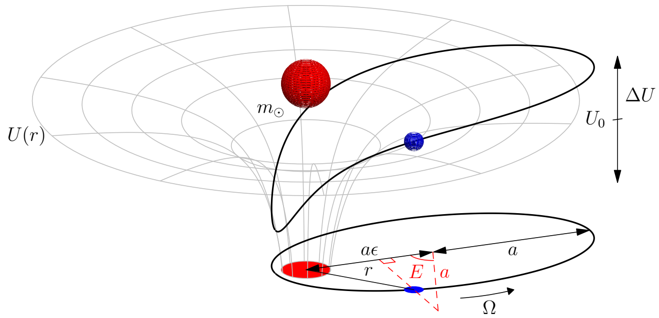

FIG. 3: (color online). Earth (blue) orbiting around Sun (red, mass $m_\odot$) in gravitational potential U on an orbit with semi-major axis a, eccentricity ϵ (exaggerated to show geometry) and angular velocity Ω. Earth is shown at radial distance r from the Sun. The eccentric anomaly E is the angle between the major axis and the orthogonal projection of Earth's position onto a circle with radius a.

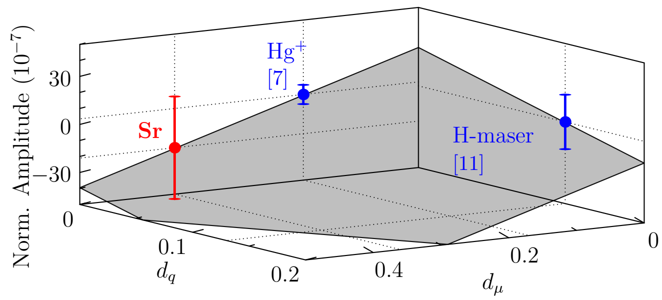

j	c_α^j	k_α	$+d_\mu^j k_\mu$	$+d_q^j k_q$	$= y_j/(c_\alpha^j u)$
Sr	2.77	k_α	$+0.36k_\mu$		$= (-2.1 \pm 3.2) \times 10^{-6}$
Hg$^+$	6.03	k_α	$+0.17k_\mu$		$= (3.5 \pm 6.0) \times 10^{-7}$
H-maser	0.83	k_α		$+0.13k_q$	$= (1 \pm 17) \times 10^{-7}$

FIG. 4: (color online). A fit to linear constraints on gravitational coupling constants k_α, k_μ and k_q from three species determines a plane. Its value at d_μ=0, d_q=0 is k_α; its gradient along the d_μ (d_q) axis is k_μ (k_q). The table shows sensitivity constants and constraints for ^{87}Sr, ^{199}Hg$^+$ and the H-maser.

For ^{87}Sr in particular, $-c_\alpha^{\rm Sr} = 0.06 - 0.83 - 2 = -2.77$ [24]. The ^{87}Sr sensitivity is about 50 times lower than that of Cs, so that our measurements are a clean test of the Cs frequency variation. This allows Sr clocks to serve a similar role as H in removing the Cs contribution from other optical clock experiments or to act as an anchor in direct optical comparisons [3].

Other optical clock species with different sensitivity constants have also been analyzed for frequency drifts. Each species becomes susceptible to variations in both α and μ by referencing to Cs. Figure 2 shows current optical frequency drift rates from Sr, Hg$^+$ [7], Yb$^+$ [6], and H [3]. Linear regression [27] limits drift rates to

$$\begin{aligned}\delta\alpha/\alpha &= (-3.3 \pm 3.0) \times 10^{-16}/\mathrm{yr} \\ \delta\mu/\mu &= (1.6 \pm 1.7) \times 10^{-15}/\mathrm{yr},\end{aligned} \tag{4}$$

decreasing the H-Yb$^+$-Hg$^+$ [3, 6, 7] errorbars [28] by $\sim$15% and confirming the null result at the current level of accuracy by adding high-accuracy data from a very insensitive species such as Sr to Fig. 2. We note that another limit on $\delta\alpha/\alpha$ independent of other fundamental constants (using microwave transitions in atomic Dy) has recently been reported as $(-2.7 \pm 2.6)\ 10^{-15}$/yr [29].

We will now generalize the formalism used for the analysis of linear drifts to constrain coupling to the gravitational potential U and search for periodic variations in the global frequency record. The dominant contribution to changes in the ambient gravitational potential is due to the ellipticity of Earth's orbit around the Sun. Suppose that the variation of a fundamental constant η is related to the change in gravitational potential via a dimensionless coupling constant k_η [9]:

$$\frac{\delta\eta}{\eta} \equiv k_\eta \frac{\Delta U(t)}{c^2}, \tag{5}$$

where $\Delta U(t) = U(t) - U_0$ is the variation in the gravitational potential versus the mean solar potential on earth U_0, and c is the speed of light.

The variation in solar gravitational potential can then be estimated from Earth's equations of motion (see Fig. 3). Since Earth's orbit is nearly circular, we expand the solar gravitational potential $U(t) = -Gm_\odot/r(t)$, with gravitational constant G, Sun mass $m_\odot$, and radial distance Earth–Sun $r(t)$, in the orbit's ellipticity $\epsilon \simeq 0.0167$. Kepler's equation [30] relates the eccentric anomaly $E \equiv \arccos[(1 - r/a)/\epsilon]$ (with semi-major axis $a \simeq 1$ au) to the orbit's elapsed phase since perihelion:

$$\Omega t = E - \epsilon \sin E, \tag{6}$$

where $\Omega \simeq \sqrt{Gm_\odot/a^3} \simeq 2 \times 10^{-7}\ \mathrm{s}^{-1}$ is Earth's angular velocity from Kepler's third law. Kepler's equation has a solution given by a power series in the ellipticity as $E = \Omega t + \mathcal{O}(\epsilon)$, which can be used to expand $1/r$ and thus ΔU to first order in ϵ:

$$\Delta U(t) = -\frac{Gm_\odot}{a}\epsilon\cos\Omega t, \tag{7}$$

with a dimensionless peak-to-peak amplitude $u \equiv 2Gm_\odot/(ac^2) \simeq 3.3 \times 10^{-10}$. Thus, the ^{87}Sr fractional frequency variation due to gravitational coupling is

$$x_{\rm Sr}(t) = [2.77k_\alpha + k_\mu]\frac{Gm_\odot}{ac^2}\epsilon\cos\Omega t, \tag{8}$$

with amplitude containing k_α and k_μ as the only free parameters. Fitting Eqn. 8 to the combined Sr frequency record in Fig. 1(b) gives an annual variation with amplitude $y_{\rm Sr} = (-1.9 \pm 3.0) \times 10^{-15}$, which constrains $2.77k_\alpha + k_\mu$ by division through u.

Other atomic clock species that have been tested for gravitational coupling are ^{199}Hg$^+$ [7] and the H-maser [11]. H-masers are also sensitive to variations in the light quark mass [25], adding a third coupling constant k_q. Although the maser operates on a hyperfine

transition, the H atom is well understood, permitting the use of H-maser data with optical clocks to constrain k_q. Using sensitivity coefficients from references [24, 25], each atomic clock species j contributes a constraint of the general form [9]

$$c_\alpha^j k_\alpha + c_\mu^j k_\mu + c_q^j k_q = y_j/u. \quad (9)$$

Division by c_α^j gives this equation the form of a linear function in two variables $d_\mu^j \equiv c_\mu^j/c_\alpha^j$ and $d_q^j \equiv c_q^j/c_\alpha^j$.

In Fig. 4, each species' constraint is interpreted as a measurement of this linear function in the numerical coefficients [32]. A linear fit gives:

$$\begin{aligned} k_\alpha &= (2.5 \pm 3.1) \times 10^{-6} \\ k_\mu &= (-1.3 \pm 1.7) \times 10^{-5} \\ k_q &= (-1.9 \pm 2.7) \times 10^{-5}. \end{aligned} \quad (10)$$

Due to the orthogonal dependence on k_q, the maser data only pivots the plane in Fig. 4 around the Hg^+–Sr line, but its value and error bar influence neither the value nor the error bar of k_α and k_μ. The values agree well with zero and we conclude that there is no coupling of α, μ and the light quark mass to the gravitational potential at the current level of accuracy. We note that the coupling constant k_α has recently been measured independently in atomic Dy, resulting in $k_\alpha = (-8.7 \pm 6.6) \times 10^{-6}$ [31], limited by systematic effects. While optical clocks are not as sensitive to variations in constants as Dy, systematic effects have been characterized at much higher levels [20].

The unprecedented level of agreement between three international labs on an optical clock frequency allowed precise analysis of the Sr clock data for long-term frequency variations. We have presented the best limits to date on coupling of fundamental constants to the gravitational potential. In addition, by adding a high-accuracy measurement of a low-sensitivity species to the analysis of drifts of fundamental constants, we have increased confidence in the zero drift result for the modern epoch.

The Boulder group thanks T. Ido, S. Foreman, M. Martin and M. de Miranda as well as T. Parker, S. Diddams, S. Jefferts and T. Heavner of NIST for technical contributions and discussions. The Paris group acknowledges contributions by P. G. Westergaard, A. Lecallier, the fountain group at LNE-SYRTE, and by G. Grosche, B. Lipphardt and H. Schnatz of PTB. The Tokyo group thanks Y. Fujii and M. Imae of NMIJ/AIST for GPS time transfer. We thank S. N. Lea for helpful discussions.

Work at JILA is supported by ONR, NIST, NSF and NRC. SYRTE is Unité Associée au CNRS (UMR 8630) and a member of IFRAF. Work at LNE-SYRTE is supported by CNES, ESA and DGA. Work at U. Tokyo is supported by SCOPE and CREST.

* Electronic address: sebastian.blatt@colorado.edu

† Permanent address: The Niels Bohr Institute, Universitetsparken 5, 2100 Copenhagen, Denmark

‡ Current address: Dept. of Physics, Columbia University, New York, NY, USA

§ Current address: Laboratoire Collisions Agrégats Réactivité, UMR 5589 CNRS, Université Paul Sabatier Toulouse 3, IRSAMC, 31062 Toulouse Cedex 9, France

¶ Current address: National Institute of Standards and Technology, 325 Broadway, Boulder, CO 80305, USA

** Permanent address: National Metrology Institute of Japan, National Institute of Advanced Industrial Science and Technology, Tsukuba, Ibaraki 305-8563, Japan

[1] S. G. Karshenboim, V. V. Flambaum, and E. Peik, in *Handbook of Atomic, Molecular and Optical Physics*, edited by G. W. F. Drake (Springer, 2005), pp. 455–463.
[2] S. N. Lea, Rep. Prog. Phys. **70**, 1473 (2007).
[3] M. Fischer *et al.*, Phys. Rev. Lett. **92**, 230802 (2004).
[4] E. Peik *et al.*, Phys. Rev. Lett. **93**, 170801 (2004).
[5] S. Bize *et al.*, J. Phys. B: At. Mol. Opt. Phys. **38**, S449 (2005).
[6] E. Peik *et al.*, arXiv:physics/0611088v1 (2006).
[7] T. M. Fortier *et al.*, Phys. Rev. Lett. **98**, 070801 (2007).
[8] P. Wolf *et al.*, arXiv:0711.0304v2 (2007).
[9] V. V. Flambaum, Int. J. Mod. Phys. A **22**, 4937 (2007).
[10] A. Bauch and S. Weyers, Phys. Rev. D **65**, 081101(R) (2002).
[11] N. Ashby *et al.*, Phys. Rev. Lett. **98**, 070802 (2007).
[12] M. M. Boyd *et al.*, Phys. Rev. Lett. **98**, 083002 (2007).
[13] X. Baillard *et al.*, Euro. Phys. J. D, published online DOI:10.1140/epjd/e2007-00330-3 (2007).
[14] G. K. Campbell *et al.*, in preparation (2008).
[15] M. Takamoto *et al.*, J. Phys. Soc. Jpn. **75**, 104302 (2006).
[16] H. Katori *et al.*, Phys. Rev. Lett. **91**, 173005 (2003).
[17] A. D. Ludlow *et al.*, Phys. Rev. Lett. **96**, 033003 (2006).
[18] R. Le Targat *et al.*, Phys. Rev. Lett. **97**, 130801 (2006).
[19] M. M. Boyd *et al.*, Science **314**, 1430 (2006).
[20] A. D. Ludlow *et al.*, arXiv:0801.4344v1, accepted for publication in Science (2008).
[21] S. M. Foreman *et al.*, Phys. Rev. Lett. **99**, 153601 (2007).
[22] M. M. Boyd *et al.*, in *20th European Frequency and Time Forum* (2006), pp. 314–318.
[23] J. Ye *et al.*, in *Atomic Physics 20, Proceedings of the XX International Conference on Atomic Physics*, edited by C. Roos, H. Häffner, and R. Blatt (2006), pp. 80–91.
[24] E. J. Angstmann, V. A. Dzuba, and V. V. Flambaum, arXiv:physics/0407141v1 (2004).
[25] V. V. Flambaum and A. F. Tedesco, Phys. Rev. C **73**, 055501 (2006).
[26] H. Marion *et al.*, Phys. Rev. Lett. **90**, 150801 (2003).
[27] M. Zimmermann *et al.*, Laser Physics **15**, 997 (2005).
[28] A. Kolachevsky *et al.*, to be published (2008).
[29] A. Cingöz *et al.*, Phys. Rev. Lett. **98**, 040801 (2007).
[30] W. M. Smart, *Celestial Mechanics* (Wiley, 1953).
[31] S. J. Ferrell *et al.*, Phys. Rev. A **76**, 062104 (2007).
[32] The constraint for Hg^+ is corrected for a sign error in applying Eqn. 2 of reference [7] in the subsequent paragraph. The sign of the constraint for the H-maser derives from the averaged fit in Fig. 3 of reference [11].